Wasit Journal for Pure Science

Journal Homepage: https://wjps.uowasit.edu.iq/index.php/wjps/index
e-ISSN: 2790-5241 p-ISSN: 2790-5233

Fabrication of a Nanocarbon-Reinforced Nanoclay Membrane for Purification of Drinking Water Contaminated with *Escherichia coli*

Batool Sh. Razij[1]*, Mohammed M. Sharqi[2] and Mazin A. Alalousi[3]

[1,2]Department of Biology, College Education for Women, University of Anbar, IRAQ

[3]Nanomaterials Research Center, University of Anbar, Ramadi, IRAQ.

*Corresponding Author: Batool Sh. Razij

DOI: https://doi.org/10.31185/wjps.829
Received 17 March 2025; Accepted 18 June 2025; Available online 30 March 2026

ABSTRACT: Ultrafiltration systems are considered clean and environmentally acceptable for removing bacteria and contaminants from drinking water. This study used poly sulfone polymer (PSU), DMF, Kaolinite Nanoclay with carbon nanoparticles synthesized from date seeds using reverse-phase technology. In this case, the performance of an ultrafiltration (UF) membrane was improved. Carbon nanoparticles (0, 0.025, 0.050, and 0.075%) were examined, and the polymer concentration was maintained at 17%. The membrane was tested for its ability to remove Escherichia coli from contaminated drinking water**.** FTIR, AFM, SEM, and EDX tests were used to characterize the membrane composition and structure. As the carbon nanoparticle concentrations varied, the membrane's morphology changed. Various factors were also studied, such as the membrane's ability to remove bacteria from drinking water. The synthesis of membrane (nanofilm) was confirmed using FTIR which conformed presence of active groups responsible for the synthesis process. AFM show revealed an array of homogeneous particles with a regular surface, SEM show a smooth spherical appearance with a diameter range of the particles between 27.69-63.74 nm, EDX spectra shown the main components of the extract were carbon (C), and oxygen (O), , with percentages of 64.8%, and 24%, respectively. The presence of minor components such as Al, Si, S, and Cl with percentages of 0.6%, 0.7%, 8.7%, and 0.3%, respectively. The results of removing contaminated bacteria from drinking water using membranes indicated significant statistical differences ($P \leq 0.05$) between the membranes. The efficiency of the membranes was in the following order: F4>F3>F2>F1 compared with sampled without treatments. The study demonstrated that the fabricated nanoclay membrane reinforced with nanocarbon exhibited high efficiency in removing *Escherichia coli* from contaminated drinking water.

Keywords: Nanotechnology, date seeds, Ultrafiltration systems, *Escherichia coli*

1. INTRODUCTION

Contaminated drinking water is one of the biggest health and environmental challenges facing the world, directly linked to high rates of infectious diseases, particularly in developing countries (1). Among the most common contaminants in surface and groundwater is the bacterium *Escherichia coli* (*E. coli*), which is a strong indicator of fecal contamination and inadequate water treatment (2, 3). Consuming water contaminated with this bacterium can lead to acute intestinal illness and, in some strains, serious complications such as hemolytic uremic syndrome (HUS) (4).

Given the serious effects of water pollution, interest has grown in recent years in developing effective water purification technologies using nano materials, due to their high surface area and excellent functional activity (5). Nanofiltration

membranes have emerged as a promising solution in this field, especially when designed to combine the properties of different materials to achieve enhanced performance (6).

In this context, nanoclay is a low-cost, highly effective natural material for removing biological and chemical contaminants from water, thanks to its layered structure and excellent adsorption properties. However, the individual performance of clay may not be sufficient to achieve high purification levels, especially for microorganisms such as bacteria (7, 8).

To enhance the mechanical and functional properties of nanoclay membranes, it has become common to combine them with carbon nanomaterials such as carbon nanotubes (CNTs) or graphene, which provide high-strength structural support as well as antibacterial properties. These materials create nanopores in bacterial cell walls and inhibit their biological activity, adding a new dimension to the membrane's effectiveness (9).

Therefore, the design of a nanocomposite membrane made of clay reinforced with nanocarbon represents an innovative and multifunctional approach to purifying drinking water from biological contaminants, most notably *E. coli* bacteria. In this research, nanocarbon was manufactured in an environmentally friendly manner using date pits as a natural carbon source, reflecting the trend toward recycling agricultural waste and applying circular economy principles to technical solutions. This approach contributes to reducing environmental and material costs and enhancing the sustainability of materials used in water purification, making the proposed system not only effective in performance but also safe and environmentally friendly.

2. MATERIALS AND METHODS

2.1 Water sample collection

Five samples of drinking water were collected from the water distribution network in Ramadi city, and one sample was used as a control without any filtration. Additionally, four other treatments were prepared, each of which was filtration using one of the nanofilters prepared in this study.

2.2 Preparation of water samples contaminated with *E.coli*

An *E. coli* isolate was activated according to the method mentioned by McCance and Harrigan (1976) (10). Nutrient broth was used according to the instructions of the supplier company. 13 g of it was dissolved in a liter of deionized water and transferred to test tubes. The bacterial isolate was added to it and transferred to an incubator at 37°C for 48 hours. After that, the filtrate was separated using a centrifuge, and the precipitate was taken and transferred to a liter of distilled water sterilized by an autoclave to ensure that it was free of microorganisms.

2.3 Collecting and Preparing Date Seeds

The seeds were collected from the Zahdi variety of dates (considered a plant waste) and cleaned by washing them thoroughly with distilled water several times to remove the stickiness. They were then soaked in warm distilled water (55°C) for several hours, ensuring cleanliness. They were then filtered through a special strainer and dried after spreading them out on a clean cloth in a sunny, well-ventilated area, stirring continuously (to ensure complete drying) for five days. Then, ground in a GM200 grinder (Retsch, GmbH, Germany), sieved to obtain a particle size fraction of 500 μm < d < 250 μm (60–35 mesh) for better decomposition in the CHTC process, and finally stored in a desiccator for later use (11).

2.4. Hydrothermal Carbonization (HTC)

The nano-carbon extract was prepared using the hydrothermal method in two stages.

2.4.1 First stage, was using an autoclave to treat 1000 gm of date seed powder with 8 L of distilled water at 130°C, 1.7 MPa for 120 minutes. After cooling, the filtration process was carried out and the filtrate was returned to the autoclave for a second time to react the materials inside the device under a pressure of 1.7 MPa and a temperature of 130°C for two hours. Then, the filtration was carried out again using a centrifuge (3000 rpm) for 20 minute and the filtrate was concentrated using a rotary evaporator under vacuum pressure. The concentrated filtrate was dried using an electric air oven at a temperature of 125°C for 24 hours.

2.4.2. Second stage, A magnetic mixer was used to mix 40g of date seed extract with 160 ml of ethanol in a one-liter glass conical flask at a temperature of 50-60C, stirring for 2-4 hours until a dark brown solution was obtained. This solution was then transferred to an autoclave and heated at a temperature of 130°C and a pressure of about 1.7 MPa for 150 minutes. After completing the autoclaving process, the solution was left to cool gradually. After the solution cooled, the solution was removed from the autoclave and the result was a dark brown solution. Then, the solution was placed in a centrifuge at a speed of 3000 rpm for 15 minutes to separate the precipitate with less fluorescence. The solution was washed using acetone by centrifugation at a high speed of 9000 rpm for 15 minutes to obtain the precipitate. The precipitate was then collected and washed with distilled water using a centrifuge at 3000 rpm for 5 minutes. The washing process was repeated three times. Sometimes a very bright luminous carbon material is obtained, and then the precipitate is dried by placing it in a glass dish in a drying oven at a temperature of 110-120°C for (4-6) hours. Then the material is ground in an electric grinder, and finally the carbon powder is obtained and stored in glass containers (12).

2.5 Preparation of the CQD/Fe_2O_3-NPs Nanocomposite

The CQD/Fe_2O_3NPs nanocomposite was prepared using a green building method. 50 mL of the CQD extract was slowly and dropwise added to a solution of ferric chloride ($FeCl_3 \cdot 6H_2O$) with continuous stirring using a magnetic stirrer at room temperature. The pH of the mixture was then adjusted to 12 by gradually adding 1 M NaOH solution. Stirring continued for 3–4 hours, resulting in redox reactions and the formation of Fe_2O_3-NPs, as evidenced by the solution turning dark black. The nanoparticles were then separated by centrifugation at 8,000 rpm for 20 minutes. The resulting precipitates were first washed with ethanol and then with distilled water several times to remove impurities. Finally, the nanoparticles were dried in an air oven at 80°C for 3 hours and then stored in a sealed container for future use(13).

2.6 Preparation of pure and composite ultrafiltration (UF) membranes

Using the phase inversion technique**,** 15 wt. % of Poly sulfone with nano clay particles (kaolin) at a ratio of 0.001% and nano carbon extracted at concentrations of 0.025%, 0.050%, and 0.075% respectively for three membranes mixed matrix ultrafiltration membranes were created. Table 1 displays the chemical compositions of each casting solution. For each of the membranes, the casting solution was made as follows. The right quantity of nano clay and nano carbon was first added to DMF. The casting solution was then magnetically agitated for 6 hours at 60 °C after PSU was added to the solutions. The casting solution was allowed to sit for 24 hours to degas. On the clean glass, a 180-micrometer of casting solution was applied using a casting Gardner knife (Filmography: film casting doctor blade). Glass and cast film were briefly submerged in DI water. The created membrane floated off the glass surface to get rid of any remaining solvent.

Before testing, membranes were maintained in DI water for at least 24 h. Monitoring revealed that the process temperature was constant at 25 °C with a 1 °C tolerance (14).

Table 1. Ultrafiltration membrane composition

Membranes Name	Casting Solution (wt.%)			
	PSU Polymer (%)	DMF wt(%)	Kaolinite Nanoclay wt(%)	Nanocarbon wt(%)
F1	15%	8.5		
F2	15%	8.5	0.001	0.025
F3	15%	8.5	0.001	0.050
F4	25%	8.5	0.001	0.075

To characterize the ultrafiltration (UF) membranes, several tests (FTIR, AFM, EDX, XRD, SEM) were conducted. The membranes were installed one by one on a locally manufactured drinking water purification device.

2.7 Characterization of membrane

UV-visible (UV-vis) spectrophotometry was conducted using an Agilent UV-Cary 60 instrument. The measurements were carried out on materials that were distributed in suspensions of glycerine and water. FTIR analysis was conducted using the IRTracer-100 instrument manufactured by Shimadzu in Japan, the powdered form was measured with a KBr disk in the wavenumber range of 4000 to 400 cm^{-1} (15). The purpose of this analysis was to identify the primary functional groups present in the biosorbent. The chemical structure and surface morphology of the biosorbent was examined using a scanning electron microscope coupled to an energy dispersive X-ray, JSM 7600F, JEOL Inc., Japan at a working voltage of 5 kV at various magnifications (16).

2.8 Total Plate Count (TPC)

The TCP was calculated using the plate counting method according to (APHA) (17). First, dilutions were made to the sample so that the number of bacteria in each plate was within the countable range (usually between 30–300) colonies. Then, 1 mL of the original sample was taken and added to a tube of sterile distilled water. The contents were mixed well. Then, a certain volume of this dilution was taken and added to another tube containing diluted liquid. Then, a series of dilutions were obtained. The sample was taken from the second dilution and added to a Petri dish containing dissolved solid nutrient agar. Then, the dish was gently rotated to distribute the sample evenly. Then, by pouring, the medium was added to the sample and left to stand. After that, the dishes were taken to an incubator set at 30°C, and the bacteria were given sufficient time and suitable conditions for growth in order to form visible colonies on each dish using a magnifying glass. Dishes containing a number of colonies ranging from 30–300 colonies were tested for calculations in order to know the number of bacteria in the original sample according to the general equation.

2.9 Statistical Analysis

The Statistical Analysis System, User's Guide (2018) program was used to detect the effect of difference factors in study parameters. Least significant difference-LSD was used to significant compare between means (ANOVA/ One way or Two way) in this study.

3. RESULTS AND DISCUSSION

3.1 FTIR Membrane Analysis

According to the results of the current study Figure (1) and Table 2, show the results of determining the chemical bonds characteristic of the peaks responsible for the stretching vibrations of the groups of carbon compounds identified in the FTIR spectra of the carbon extract showed most of the frequency peaks in the extract, indicating the efficiency of preparing the carbon extract, as alkanes, alkenes, aromatic cyclic compounds, alkyl halides, and aliphatic amines were obtained, while after converting them to nanoparticles, new frequencies appeared (947, 3402, and 3751) cm^{-1}, which indicate the extension = C-H bend, N-H stretch, and O-H stretch, free hydroxyl, which could be alkenes, amines, amides, alcohols, and phenols, respectively. While a number of frequencies disappeared after preparing the nanoparticles after they were apparent in the carbon extract, namely frequencies (1278, 1375, 1521, 1610 and 1869) cm^{-1}, which indicate C-N stretch, C-H rock, N-O asymmetric stretch and N-H bend, and indicate the appearance of aliphatic amines, nitrite compounds, amines and carbonyl compounds, respectively(18), which can occur as a result of reactive bonds and by oxidation and reduction processes and the appearance of new binding sites(19), which confirms the results of good preparation of nanoparticles and their stability. On the other hand, these extensions appeared in the carbon extract and nanoparticles in the samples of nanofilters prepared from nanoparticles of the carbon extract and nanoclay compounds added to the filters through a mixing process between the nanocomposites in order to obtain nanofilters effective in achieving the purpose for which they were prepared, which is the biological and chemical treatment of polluted water.

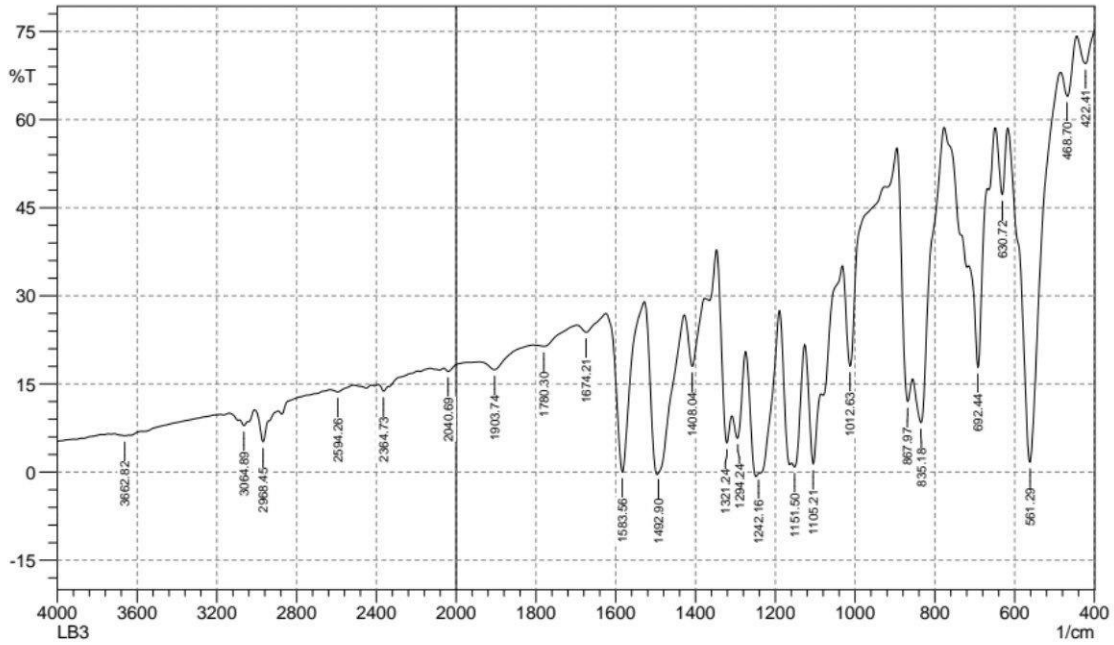

Figure 1. FTIR of membrane

Table 2. FTIR analysis results of nanofilters

No.	Nano filter		
	Peak	**bond reaction**	**Compound**
1	561	C-Br	Alkyl halides
2	630	- C=C-H; C-H bend	Alkynes
3	692	- C=C-H; C-H bend	Alkynes
4	835	C-Cl stretch	Alkyl halides
5	867	C-H OOP	Aromatics
6	1012	C-N stretch	Aliphatic amines
7	1105	C-N stretch	Aliphatic amines
8	1151	C-N stretch	Aliphatic amines
9	1242	C-N stretch	Aliphatic amines
10	1294	C-H wag (-CH2X)	Alkyl halides
11	1321	C-N stretch	Aromatic amines
12	1408	C-C stretch (in ring)	Aromatic
13	1492	C-C stretch (in ring)	Aromatic
14	1583	C-C stretch (in ring)	Aromatic
	1674	-C=C- stretch	Alkenes
	1780	C=O stretch	carbonyls
	1903	-C=C- stretch	Alkynes
	2040	-C=C- stretch	Alkynes
	2364	C=N stretch	nitriles
	2594	H-C=O; C-H stretch	Aldehyde
	2968	C-H stretch	Alkanes
	3064	=C-H stretch	Alkenes
	3662	O-H stretch, free hydroxyl	Alcohol; phenols

3.2 AFM Analysis

Atomic force microscopy (AFM) images were used to measure the particle size and surface topography of the nanofilms. Figure (2) shows the two-dimensional and three-dimensional images of the carbon- and nanoclay-loaded nanofilms, which revealed an array of homogeneous particles with a regular surface shape. AFM images showed good geometric symmetry between the carbon and nanoclay-loaded nanofilms, resulting in the formation of well-aligned individual clusters. From the information contained in the image, the root mean square (RMS) values of 12.343 nm and the average surface roughness of 31.83 nm were calculated, which provided information about the minimum and

maximum coverage area, which amounted to 8.89-11.61 nm Figure (2). Our results differ from what Rosales *et al*. (2024) reported that the transmission electron microscope (AFM) images determined the morphology of the crystals, which appeared as parallel lines, forming circular structures confirming the presence of single spherical nanocrystals(20). Our results were consistent with the study of Su *et al.* (2018) that these structures are present in nanocarbon, which showed that nanocarbon is a zero-dimensional nanomaterial with diameters ranging between 1 and 20 nm. Statistical analysis of the microscopic images allowed the calculation of the average diameters of green CQD, red CQD, and blue CQD as (8.5, 5.7, and 3.9) nm, respectively(21). These studies revealed thicknesses ranging from 1–20 nm, with defects in the crystal structure of the material being linked to its photoemission ability.

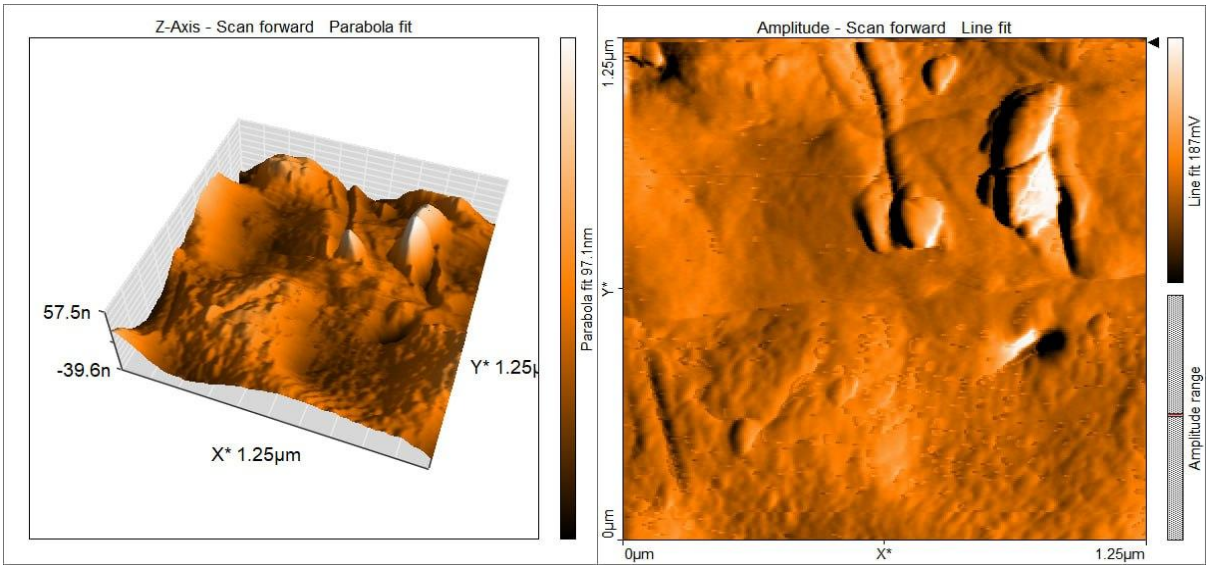

Figure 2. 2D and 3D images of nano-films

3.3 FE-SEM Analysis

Scanning electron microscope is an effective technique for analyzing materials on a scale from nanometer to micrometer (µm), whether organic or inorganic. The shapes, sizes and nature of the surface structure of the prepared carbon nanoparticles and nanofilms were revealed using SEM. The results shown in Figure (3 A and B), Figure 3A showed a smooth spherical appearance with the average particle diameter was found to be 27.69 to 63.74 nm, and relatively homogeneous in appearance and Figure 3B show Nano prose of nanofilm. From a study conducted by Anand Raj *et al*. (2015) to detect nanoparticles containing bovine serum albumin using a scanning electron microscope, to confirm the dimensions and shape of the nanoparticles, the nanoparticles appeared spherical in shape with an average nano size of 96 nm (22).

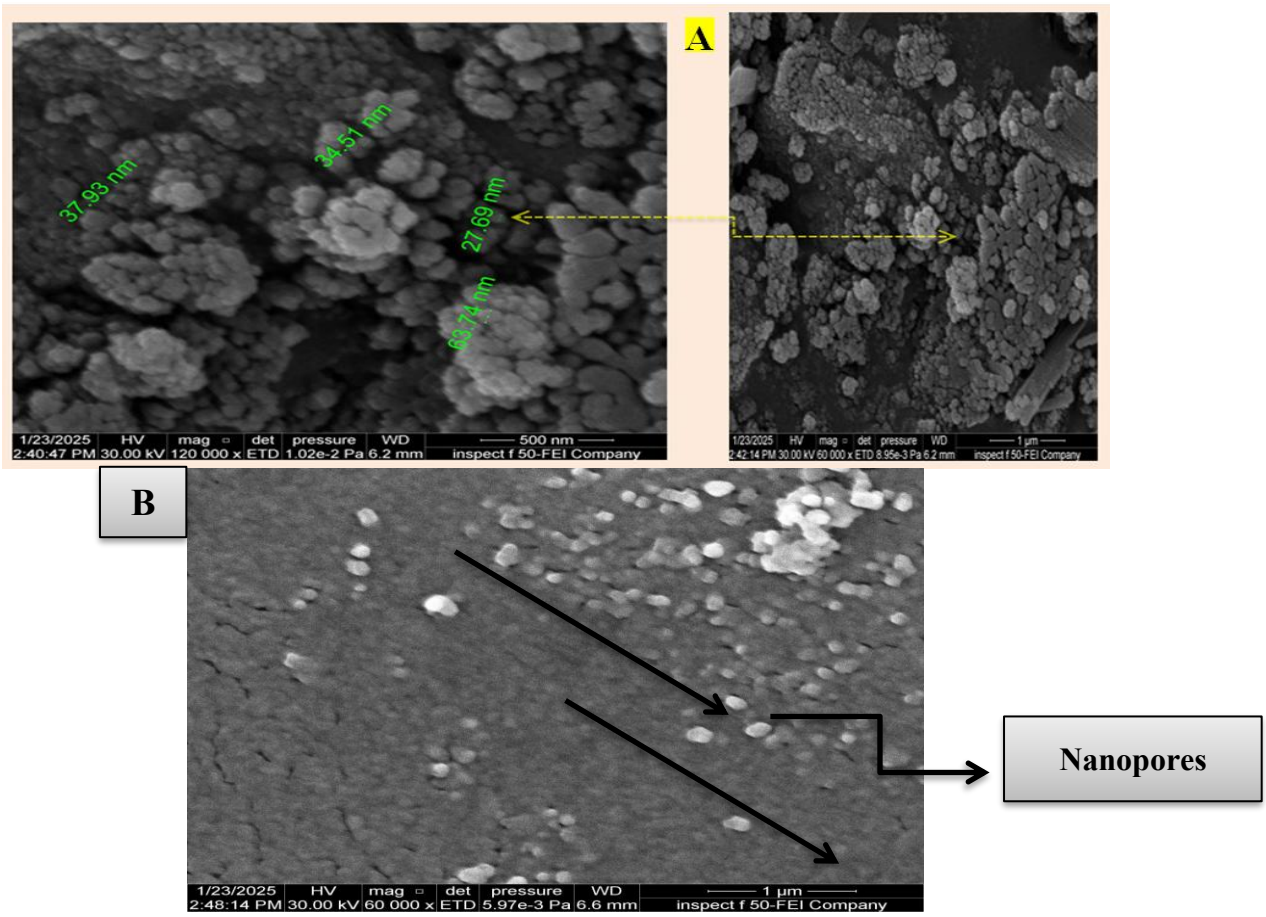

Figure 3. SEM analysis of nano-film

3.4 EDX Analysis

Elemental analysis of the prepared nano-membranes of carbon and nano-clay was carried out using EDX technique, as shown in Table (3) and Figure (4). The results showed that the majority of atoms was found to be 64.8%, as carbon atoms and 24% as oxygen atoms respectively. The presence of minor components such as Al, Si, S, and Cl with percentages of 0.6%, 0.7%, 8.7%, and 0.3%, respectively, confirmed that the presence of chlorine and aluminum salts and low concentrations of the remaining elements indicate the presence of carbon extract. When compared with the EDX analysis results of the nanofilms prepared from nanocarbon and nanoclay, the results confirm the presence of nanocarbon and nanoclay, as the weight percentages of carbon and oxygen are higher than in nanocarbon, and there is a discrepancy between the percentages of other elements, indicating the presence of nanoclay and nanocarbon in the nanofilms. Our results are consistent with what was reported by Abul Hossain and Islam (2013), as the EDX analysis reveals the presence of pure carbon without any contamination, which is indicated by the X-ray diffraction analysis of the prepared carbon nanoparticle powder, which indicates the presence of large quantities of amorphous carbon material associated with the hexagonal graphite network. FTIR spectroscopy shows that the prepared carbon nanoparticles are a mixture of elemental carbon and a small number of hydrocarbons. This was confirmed by the study of Abul Hossain and Islam (2022), which showed the appearance of non-uniform size of carbon nanoparticles, most of which were spherical and their diameters ranged between 10 and 70 nm (23). The composition of carbon particles was confirmed by EDX analysis. Most of the amorphous carbon materials, in addition to some hexagonal crystal lattice of graphite, were identified by XRD analysis.

Table (3) EDX analysis of nano-membranes prepared from carbon and nano-clay

No.	Metals	Weight (%)
1	C	64.8
2	O	24.0
3	Al	0.6
4	Si	0.7
5	S	8.7
6	Cl	0.3
7	Fe	0.9

4.

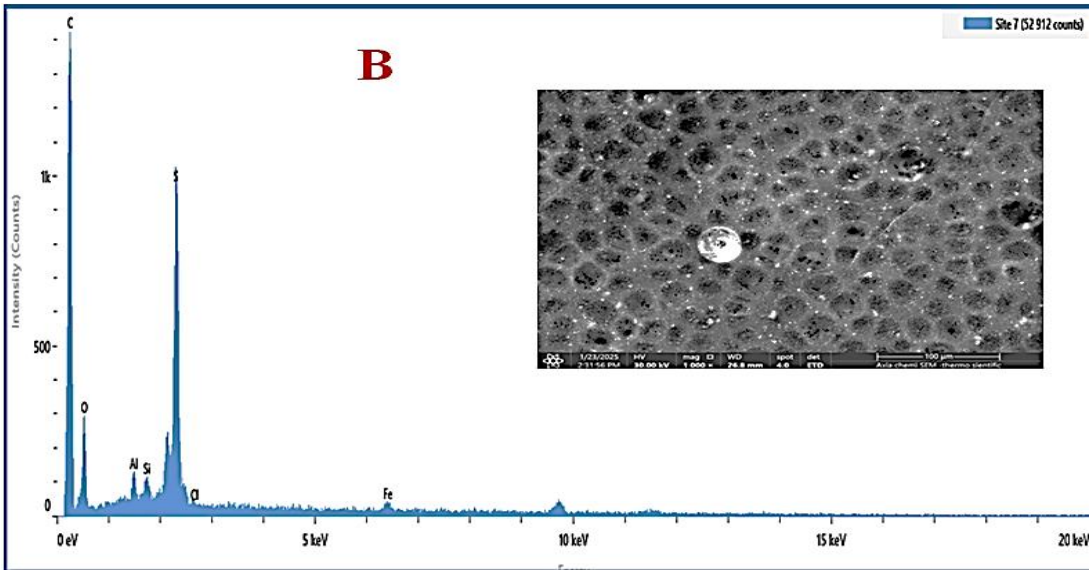

Figure 4. EDX results of the nanofilms.

Table 3, shows the total bacterial count (TBC) of water samples contaminated with *E. coli* after filtration using different nano-membranes (F1 to F4), along with a control sample (C) without any filtration. The results in Table (4) demonstrate the effect of the nanomembranes on reducing the total bacterial count in the *E. coli*-contaminated water samples, compared to the untreated treatment (C). Treatment C recorded the highest bacterial count, reaching 71.5×10^6 CFU/ml, indicating the severity of bacterial contamination in the original samples prior to treatment and highlighting the urgent need for effective technologies to purify water from these harmful microorganisms.

When using nano-membranes, a significant decrease in bacterial counts was observed, demonstrating the membranes' effectiveness in removing *E. coli*. Membrane F1 recorded a bacterial count of 107.5×10^3 CFU/ml, a significant decrease compared to the control, but still higher than the other membranes, suggesting that its filtration efficiency was relatively limited. Membrane F2 recorded a lower count of 89.5×10^3 CFU/ml, indicating a significant improvement in its ability to reduce bacterial contamination.

Membrane efficiency continued to improve with the use of membrane F3, with the count decreasing to 71×10^2 CFU/ml, reflecting improvements in membrane design or properties that contributed to its increased effectiveness. The best results were achieved with membrane F4, which recorded the lowest bacterial count of 48×10^2 CFU/ml, indicating that it was the most efficient at removing bacteria among all the membranes used in the study. These clear differences between treatments indicate that the effectiveness of nano-membranes varies depending on their type or composition, possibly due to differences in pore size or the nature of the nanomaterial used in manufacturing. This conclusion is reinforced by the presence of a significant difference between the values, as the value of (L.S.D) reached 12.305 at the probability level ($P \leq 0.05$), which means that the differences between the treatments are statistically significant

Table 4. Total bacterial count of water samples contaminated with *E. coli* filtered through nano-membranes

Treatments	Number of cell (CFU/ml)
C	$71.5 *10^6$
F1	$107.5 *10^4$
F2	$89.5 *10^3$
F3	$71 *10^2$
F4	$48 *10^2$
L.S.D.	12.305 *
	* (P≤0.05).

The highest removal rate was achieved with the F4 membrane, which combined the highest percentage of nanocarbon (0.075%) with a significantly higher concentration of the PSU polymer (25%). This combination gave the membrane dual properties: a denser structure that reduces pore size and the presence of an effective nanomaterial with antibacterial properties. As a result, F4 recorded the lowest bacterial count of 48 x 10^2 CFU/ml, demonstrating the highest filtration efficiency among all membranes.

These results support that the effectiveness of nanoporous membranes in removing bacteria is directly related to their internal composition. The higher the percentage of nanocarbon, the greater the membrane's ability to absorb and interact with bacterial cells, weakening their activity or preventing their passage. Increasing the polymer concentration also helped reduce the membrane's permeability to large molecules such as bacteria, contributing to its increased effectiveness.

Table 5: Total Bacterial Count in Tap Water Samples Filtered Through Nano-membranes

Treatments	Undiluted	First Dillution
C	310	$209 *10^1$
F1	248	$89 *10^1$
F2	184	$19 *10^1$
F3	120	$17 *10^1$
F4	17	$0.5 *10^1$
L.S.D.	22.47 *	15.62 *
	* (P≤0.05).	

Table (4) shows the total bacterial count of tap water samples filtered through nano-membranes, The results in Table (4) showed that the bacterial count in tap water gradually decreased when using nano-membranes compared to the control treatment (C). Sample C recorded the highest bacterial count, reaching 310 CFU/ml without dilution and 209 × 10^1 CFU/ml upon first dilution, reflecting moderate bacterial contamination in tap water before treatment. With the use of membrane F1, the count decreased to 248 CFU/ml without dilution and 89 × 10^1 after dilution. Despite the improvement, the membrane was not highly effective. This is attributed to the F1 formulation, which is free of nanocarbons and relies only on 15% PSU polymer and 8.5% DMF.

Results improved further with membrane F2, with the count decreasing to 184 and 19 × 10^1, respectively. This is attributed to the introduction of 0.025% nanocarbon, which added antibacterial properties to the membrane. Efficiency continued to improve with the F3 membrane, which contained a higher nanocarbon content (0.050%), with counts dropping to 120 and 17 × 10^1. The best results were achieved with the F4 membrane, which featured a robust formulation comprising 25% PSU polymer and 0.075% nanocarbon, with bacterial counts dropping to 17 CFU/ml and 0.5 × 10^1 after dilution. The results demonstrate that increasing the nanocarbon content, along with increasing the polymer concentration, improved the membranes' ability to remove bacteria by enhancing this effect is mainly attributed to the

structural and physical properties of the nanofilms, which include porosity, surface charge, and surface roughness, in addition to the effect of added nanomaterials (24). The mean significant differences (LSD) also confirm that the performance differences between the membranes are real and statistically significant. The results of this study are consistent with a study Hasan *et al*.,2022 in which polysulfone polymer (PSU) was used with silicon dioxide nanoparticles by phase reversal. In this case, the performance of the ultrafiltration (UF) membrane was improved, increasing its dye removal efficiency (14). Previous studies indicate that the incorporation of nanomaterials such as nanocarbon or nanoclay into membranes has improved their efficiency in removing bacterial contaminants from drinking water. For example, one study developed cellulose nanofiber-based membranes incorporated with activated carbon, which successfully removed Escherichia coli with high efficiency, demonstrating the effectiveness of nanocarbon in incorporating materials in improving bacterial retention capacity (25). Another study demonstrated that reinforcing thin-film composite (TFC) membranes with modified organic nanoclays helped improve water permeability and separation properties, further strengthening the role of nanoclays as an effective structural component in membranes (26).

5. CONCLUSION

The study demonstrated that the fabricated nanoclay membrane reinforced with nanocarbon exhibited high efficiency in removing Escherichia coli from contaminated drinking water. The synergistic effect between the adsorption capacity of nanoclay and the antimicrobial activity of nanocarbon significantly enhanced the bacterial removal process. The results suggest that the developed membrane can be a cost-effective, eco-friendly, and sustainable solution for water purification, particularly in areas lacking access to safe drinking water. Further research is recommended to scale up the membrane for industrial applications and assess its long-term stability and regeneration capacity.

REFERENCES

[1] Schweitzer L, Noblet J. Water contamination and pollution. Green chemistry: Elsevier; 2018. p. 261-90. http://dx.doi.org/10.1016/B978-0-12-809270-5.00011-X

[2] Liu Q, Liu M, Liu J. Association of drinking water services with the disease burden of diarrhea in children under five in 200 countries from 2000 to 2021. Cell Reports Sustainability. 2024;1(9).

[3] SHARQI MM, AL-TAMIMI A-NA, HASSAN OM. Evaluation of Euphrates River Water Quality on Phytoplankton Biodiversity in Ramadi, Iraq. https:doi.org/10.33736/bjrst.6858.2024

[4] Kwikima M. Analyzing the presence of microbial contaminants in water sourced from shallow wells within Dodoma city, Tanzania. International Journal of Energy and Water Resources. 2025;9(1):1-12. https://doi.org/10.1007/s42108-024-00278-z

[5] Wang L, Yuan Z, Karahan HE, Wang Y, Sui X, Liu F, et al. Nanocarbon materials in water disinfection: state-of-the-art and future directions. Nanoscale. 2019;11(20):9819-39.

[6] Silva M, Felgueiras H, De Amorim M. Carbon based membranes with modified properties: Thermal, morphological, mechanical and antimicrobial. Cellulose. 2020;27:1497-516. https://doi.org/10.1007/s10570-019-02861-8

[7] Kolya H, Kang C-W. Next-generation water treatment: Exploring the potential of biopolymer-based nanocomposites in adsorption and membrane filtration. Polymers. 2023;15(16):3421. https://doi.org/10.3390/polym15163421

[8] Díez-Pascual, A. M. (2021). Carbon-based nanomaterials. International Journal of Molecular Sciences, 22(14), 7726. https://doi.org/10.3390/ijms22147726

[9] Xin Q, Shah H, Nawaz A, Xie W, Akram MZ, Batool A, et al. Antibacterial carbon-based nanomaterials. Advanced Materials. 2019;31(45):1804838. https://doi.org/10.1002/adma.201804838

[10] Harrigan W, McCance M. Statistical methods for the selection and examination of microbial colonies. Laboratory methods in food and dairy microbiology. 1976:47-9.

[11] El Ouadrhiri F, Elyemni M, Lahkimi A, Lhassani A, Chaouch M, Taleb M. Mesoporous carbon from optimized date stone hydrochar by catalytic hydrothermal carbonization using response surface methodology: application to dyes adsorption. International Journal of Chemical Engineering. 2021;2021(1):5555406. https://doi.org/10.1155/2021/5555406

[12] Jabbar MS, Mahmood OA, Jameel ZN, Jihad NJ. Synthesis and photocatalytic applications of TiO2-CQDs nanocomposites prepared by biological methods. Baghdad Science Journal. 2024. https://doi.org/10.21123/bsj.2024.9549

[13] Abusalem M, Awwad A, Ayad J, Rayyan AA. Green Synthesis of α-Fe 2 O 3 Nanoparticles Using Pistachio Leaf Extract Influenced Seed Germination and Seedling Growth of Tomatos. Jordan Journal of Earth & Environmental Sciences. 2019;10(3).

[14] Hassan M, Abudi Z, Al-Furaiji M. Polysulfone ultrafiltration membranes embedded with silica nanoparticles for enhanced dye removal performance. Progress in Color, Colorants and Coatings. 2023;16(2):165-79. https://doi.org/10.30509/pccc.2022.167016.1185

[15] Chi NTL, Narayanan M, Chinnathambi A, Govindasamy C, Subramani B, Brindhadevi K, et al. Fabrication, characterization, anti-inflammatory, and anti-diabetic activity of silver nanoparticles synthesized from Azadirachta indica kernel aqueous extract. Environmental Research. 2022;208:112684. https://doi.org/10.1016/j.envres.2022.112684

[16] Essien EA, Kavaz D, Solomon MM. Olive leaves extract mediated zero-valent iron nanoparticles: synthesis, characterization, and assessment as adsorbent for nickel (II) ions in aqueous medium. Chemical Engineering Communications. 2018;205(11):1568-82. https://doi.org/10.1080/00986445.2018.1461089

[17] Association APH. Standard methods for the examination of water and wastewater: American public health association.; 1926.

[18] Kamath SV, Mruthunjayappa MH, Mondal D, Kotrappanavar NS. Nanocomposite-based high-performance adsorptive water filters: recent advances, limitations, nanotoxicity and environmental implications. Environmental Science: Nano. 2022;9(7):2320-41. https://doi.org/10.1039/D2EN00155A

[19] Joseph TM, Al-Hazmi HE, Śniatała B, Esmaeili A, Habibzadeh S. Nanoparticles and nanofiltration for wastewater treatment: From polluted to fresh water. Environmental research. 2023;238:117114. https://doi.org/10.1039/D2EN00155A

[20] Rosales S, Zapata K, Cortes FB, Rojano B, Diaz C, Cortes C, et al. Simultaneous detection of carbon quantum dots as tracers for interwell connectivity evaluation in a pattern with two injection wells. Nanomaterials. 2024;14(9):789. http://dx.doi.org/10.1016/B978-0-12-809270-5.00011-X

[21] Su A, Wang D, Shu X, Zhong Q, Chen Y, Liu J, et al. Synthesis of fluorescent carbon quantum dots from dried lemon peel for determination of carmine in drinks. Chemical Research in Chinese Universities. 2018;34:164-8. https://doi.org/10.1007/s40242-018-7286-z

[22] Raj LA, Jonisha R, Revathi B, Jayalakshmy E. Preparation and characterization of BSA and chitosan nanopartices for sustainable delivery system for quercetin. Journal of Applied Pharmaceutical Science. 2015;5(7):001-5. DOI: 10.7324/JAPS.2015.50701

[23] Hossain MA, Islam S. Preparation of Carbon Nanoparticles from Candle and Their Characterization by Advanced Spectroscopic Methods. Dhaka University Journal of Science. 2022:212-7. https://doi.org/10.3329/dujs.v69i3.60032

[24] Bernstein R, Belfer S, Freger V. Bacterial attachment to RO membranes surface-modified by concentration-polarization-enhanced graft polymerization. Environmental science & technology. 2011;45(14):5973-80.

[25]. da Silva, T. L., Alves, D. R., Pacheco, T. T., & Andrade, L. S. Membranes based on cellulose nanofibers and activated carbon for removal of Escherichia coli bacteria from water. Environmental Science and Pollution Research. 2019; 26(22), 22511–22521. https://doi.org/10.1007/s11356-019-05411-z

[26] Gautam, R., & Nema, A. K. Organically modified nanoclay filled thin-film nanocomposite membranes for reverse osmosis application. Desalination and Water Treatment. 2021; 217, 167–178. https://doi.org/10.5004/dwt.2021.26689